Non-Precipitating Stratus Cloud Images Retrieval and Characterization Using a Ground-Based Dual-Wavelength Millimeter Doppler Radar

Nivia Colón-Díaz[*a], Sandra L. Cruz-Pol[*a], Stephen M. Sekelsky[**b]
[a]Center for CLoud Microwave Measurements of ATmospheric Events; Dept. of Electrical Engineering, Univ. of Puerto Rico at Mayaguez, [b]Microwave Remote Sensing Laboratory, Dept. of Electrical Engineering, Univ. of Massachusetts at Amherst

ABSTRACT

Characterization of the microphysical properties of non-precipitating stratus clouds including their suspended-water droplet size distribution and the cloud's liquid water content are estimated in this work. The dual wavelength ratio, DWR, and the differential extinction, DE, were computed at two millimeter frequencies, 33 GHz and 95 GHz, using UMass Cloud Profiling Radar System (CPRS) to estimate the drop size distribution. Radiosonde data is used as input in a recently calibrated model for estimation of the gaseous attenuation at K_a.-band and Liebe's model at W-band. Integrated specific humidity from a radiometer is used to constrain the radiosonde specific humidity. The radar reflectivity is corrected to take into account the effect of the wind speed, the difference of beamwidth at both frequencies and the difference in sampled range cells. Radar reflectivity and ancillary data are combined to obtain the differential extinction and the estimated cloud's liquid water density. Profiles of the processed data, such as DE, the DWR and the cloud's liquid water density are presented. Cloud's water density and radar reflectivity were used for the size distribution estimation of the suspended water droplets and the effective drop diameter.

Keywords: Reflectivity, drop size distribution, cloud's liquid water density

I. INTRODUCTION

Stratus clouds frequently cover much of the sky and play a key role in keeping Earth's surface warm. They are described as visible aggregates of minute droplets of water [1]. Clouds provide an indication of what is happening in the atmosphere.

Radars or active remote sensing operating on millimeter waves have been used to study the microphysical properties of clouds [2] because they provide very fine vertical resolution compared to passive remote sensing, i.e., radiometers [5]. Ground-based radars such as the Cloud Profiling Radar System, CPRS, [2] developed by the University of Massachusetts that works on the 33 GHz (λ_o = 9.09 mm, K_a band) and 95 GHz (λ_o = 3.157 mm, W band) is employed in this work to characterize properties such as particle size estimation [3]. Because the 95 GHz channel experiences more extinction than the 33 GHz channel, a parameter called dual wavelength ratio or DWR is used. This parameter is the difference in reflectivity (33 GHz and 95 GHz) from the object under study. Another parameter used is the differential extinction, DE, which is the difference in cloud extinction rates with altitude at two different frequencies [4]. The Rayleigh approximation is used because the suspended water droplets as well as the particles on the atmosphere are much smaller than the wavelength of both frequencies.

[*] Alexa@ece.uprm.edu; SandraCruzPol@ieee.org; phone 1 787 832-4040 x2444; www.ece.uprm.edu/~pol; CLoud Microwave Measurements of ATmospheric Events (CLiMMATE); Electrical and Computer Engineering Department; University of Puerto Rico, Mayaguez Campus, Puerto Rico 00681-9042;
[**] Sekelsky@mirsl.ecs.umass.edu; phone 1 413 545-4217 ; Microwave Remote Sensing Laboratory (MiRSL); University of Massachusetts, Amherst, MA 01003

The data for this study was obtained from the 2000 Cloud IOP experiment, which was held at the DOE SGP CART Site, Lamont, OK, in the spring of 2000. Radar scans of cloud reflectivity using the CPRS were gathered from low non-precipitating stratus clouds. The data was processed and analyzed using the Interactive Data Language, IDL [6]. Radar reflectivity was corrected by wind, beamwidth and range gate. Radiosonde data was used as input to obtain the atmospheric attenuation due to water vapor [6-7] and oxygen [8]. The attenuation due to suspended water droplets is modeled with [9]. The cloud's water density can be estimated because there is a relation between reflectivity of a cloud with its water concentration [10] as well as the extinction produced by the suspended water droplets. After this, the effective drop size diameter, concentration and drop size distribution were estimated using Newton's iterative method for nonlinear equations [10].

1. BACKGROUND ATMOSPHERIC ATTENUATION MODELS

Radar reflectivity data, (Z_{33} and Z_{95}), from the CPRS, radiosonde data (pressure, height, temperature and specific humidity), and microwave radiometer data (specific humidity), were processed, analyzed and fused using IDL software. The radiosonde and the microwave radiometer data are used as inputs to model for water vapor absorption, Liebe model is used for W-band and a newer calibrated model is used for K_a-band [6-7,11-13].

1.1 Atmospheric Attenuation Models

1.1.1 Water Vapor Absorption Estimation

The water vapor absorption model is described below. Three parameters used for K_a-band are; C_L, C_W and C_C, 1.064, 1.066, 1.234 respectively for scaling the water vapor's line strength, the line width and the continuum, respectively [6-7,13]. For W-band are; CL, CW and CC, 1.0, 1.0, and 1.2, respectively.

The correction due to gaseous attenuation was made using

$$\alpha_{water} = 0.182 f^2 [T_L T_S + T_C] \tag{1}$$

where T_L, T_S and T_C refer the line strength, the line shape and continuum terms,

$$T_L = 0.0109 C_L P_{H2O} \theta^{3.5} e^{(2.143(1-\theta))} \tag{2}$$

$$T_S = \frac{\gamma}{f_z}\left[\frac{1}{(f_z - f)^2} + \frac{1}{(f_z + f)^2 + \gamma^2}\right] \tag{3}$$

$$T_C = C_C (1.13\times10^{-8} P_{H2O} P_{dry} \theta^3 + 3.57\times10^{-7} P_{H2O}^2 \theta^{10.5}) \tag{4}$$

where f is the frequency in GHz, f_z is the water vapor resonant frequency, 22.235 GHz, θ=300/(T+273.15), T in Celsius, P is air pressure in mbar, P_{H2O} is water vapor partial pressure and $P_{dry} = P - P_{H2O}$.

1.1.2 Oxygen Absorption Estimation

The oxygen absorption coefficient in air is estimated using the oxygen absorption complete solution from [8]. An adjustable parameter for the oxygen model is used, C_x, and it's equals to 1.074.

$$K_{O_2}(f) = 1.61\times10^{-2} f^2 \left(\frac{P}{1013}\right)\left(\frac{300}{T}\right)^2 F' \tag{5}$$

where f is frequency (GHz), P is atmospheric pressure (mbar), and T is atmospheric temperature (K).

$$F' = \frac{0.7\gamma_b}{f^2 + {\gamma_b}^2} + \sum_{\substack{N=1 \\ Nodd}}^{39} \Phi_N [g_{N^+}(f) + g_{N^+}(-f) + g_{N^-}(f) + g_{N^-}(-f)] \tag{6}$$

Function F' estimates the shape of the absorption spectrum and the line strengths.

$$g_{N^\pm}(f) = \frac{\gamma_N (d_{N^\pm})^2 + P(f - f_{N^\pm}) Y_{N^\pm}}{(f - f_{N^\pm})^2 + \gamma_N^2} \tag{7}$$

$$\Phi_N = 4.6 \times 10^{-3} \left(\frac{300}{T}\right)(2N+1) \times \exp\left[-6.89 \times 10^{-3} N(N+1)\frac{300}{T}\right] \tag{8}$$

$$\gamma_N = 1.18\left(\frac{P}{1013}\right)\left(\frac{300}{T}\right)^{0.85} \tag{9}$$

$$\gamma_b = 1.18\left(\frac{P}{1013}\right)\left(\frac{300}{T}\right)^{0.89} \tag{10}$$

$$d_{N^+} = \left[\frac{N(2N+3)}{(N+1)(2N+1)}\right]^{0.5} \tag{11}$$

$$d_{N^-} = \left[\frac{(N+1)(2N-1)}{N(2N+1)}\right]^{0.5} \tag{12}$$

Where γ_N, γ_b, d_{N+}, and d_{N-} are the resonant and nonresonant linewidth parameters, the amplitudes of the f_{N+} and the F_{N-} lines, respectively, and their values are given in [8].

1.2 Radar Reflectivity Data Processing and Products

1.2.1 Dual Wavelength Ratio

The dual wavelength ratio is calculated from the radar reflectivity and it's an indication of the amount and size of hydrometeors.

$$DWR = 10\log\left(\frac{Z_{33}}{Z_{95}}\right) \text{ [dB]} \tag{13}$$
$$= Z_{33dBZ} - Z_{95dBZ}$$

The 95 GHz frequency experiences more extinction than 33 GHz. This is used to estimate the microphysical properties from liquid clouds.

1.2.2 Differential Extinction

The differential extinction represents the difference in cloud extinction rates within the range cell at 95 GHz and 33 GHz

$$DE(r_0) = \left(\frac{Z_{33}(r_0 + \Delta r) 10^{Ag,33dB(r_0+\Delta r)}}{Z_{95}(r_0 + \Delta r) 10^{Ag,95dB(r_0+\Delta r)}}\right) \times \left(\frac{Z_{95}(r_0) 10^{Ag,95dB(r_0)}}{Z_{33}(r_0) 10^{Ag,33dB(r_0)}}\right) \times \left(\frac{1}{\Delta r}\right) \tag{14}$$

where A_g is the two-way attenuation due to atmospheric gases,

$$A_g(r_0) = 2\int_0^{r_0} k_g(r)dr \tag{15}$$

k_g is the gaseous extinction rate (oxygen attenuation and water vapor attenuation), r_0 is the distance to the center of the range resolution cell and Δr is the length of the resolution cell, $\Delta r = 0.075$ in kilometers. DE is also an indirect measurement of amount of suspended water droplets and therefore is useful in estimating the drop size distribution.

$$Z_{dBZe,33} = 10\log Z_{33} \tag{16}$$

$$Z_{dBZe,95} = 10\log Z_{95}$$

1.2.3 Cloud's Liquid Water Density or Liquid Water Content

The suspended water droplet reflectivity is estimated by using the Liebe's Model [9]. The attenuation due to the liquid suspended within the cloud can be obtained by using:

$$N_W{}'' = W(9/2)[\varepsilon''(1+\eta^2)]^{-1} \tag{17}$$

Where W is the liquid water content.

$$\eta = \frac{2+\varepsilon'}{\varepsilon''} \tag{18}$$

$$\varepsilon''(f) = (\varepsilon_0 - \varepsilon_1) f / f_p[1+(f/f_p)^2] + (\varepsilon_1 - \varepsilon_2) f / f_s[1+(f/f_s)^2]$$
$$\varepsilon'(f) = (\varepsilon_0 - \varepsilon_1)/[1+(f/f_p)^2] + (\varepsilon_1 - \varepsilon_2)/[1+(f/f_s)^2] + \varepsilon_2 \tag{19}$$

$$\varepsilon_0 = 77.66 + 103.3(\theta - 1)$$
$$\varepsilon_1 = 5.48 \tag{20}$$
$$\varepsilon_2 = 3.51$$

$$f_p = 20.09 - 142(\theta - 1) + 294(\theta - 1)^2$$
$$f_s = 590 - 1500(\theta - 1) \tag{21}$$

A look up table was generated for a given air temperature, differential extinction [14] and attenuation coefficients from the suspended water droplets from the Liebe [9]. The liquid water content is then computed using this table and the measured data.

2. CLOUD PROFILING RADAR SYSTEM (CPRS) AND DATA PROCESSING

Radar scans of cloud reflectivity were obtained using CPRS. This portable ground based polarimetric radar works as two independent subsystems at two different frequencies, 33 GHz (K_a Band, λ = 9.09 mm) and 95 GHz (W Band, λ =3.157 mm). The use of these two frequencies provides additional information about the hydrometeors that is not available from single frequency radars.

The 2000 Cloud IOP experiment took place in the SPG Cart Site, Lamont, Oklahoma during the Spring 2000. Data from non-precipitating stratus clouds was gathered; therefore the particles within the clouds are small

enough to assume a Rayleigh approximation (radius ≤ 50 μm). Several microphysical properties, such as the liquid water content, the drop size distribution, the peak number concentration, from stratus clouds can be derived from dual wavelength measurements.

2.1 Research Flow Diagram

The following flowchart shows the order of the processing done on the radar and ancillary data sets. Each step is described in the previous sections.

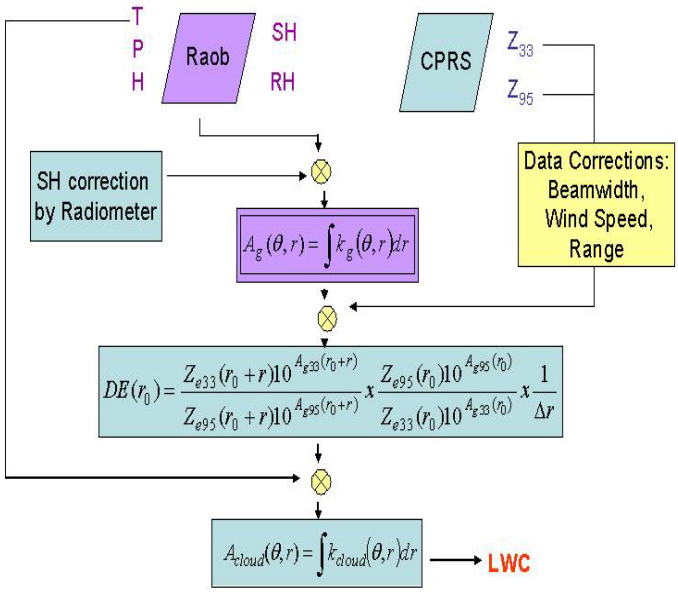

Fig. 1: Research Flow Diagram.

2.2 Scan Profiles

Radar reflectivity file of March 17th 2000, was obtained from the CPRS and visualized with IDL. As seen in Figure 2, there are two layers of stratus clouds at low elevations of less than 3 km. The clouds appear larger at 33 GHz because there is less extinction of signal by the atmosphere and therefore can "see" better. At a scanning angle of about 78 degrees from the horizon, we graphed several products such as 33 GHz and 95 GHz reflectivity, the dual wavelength ratio, the differential extinction, and the liquid water content for the data of March 17th 2000

In the Figures 3(a) to 3(d) we can see the resulting products obtained from the CPRS radar reflectivity processing after correcting by gaseous attenuation. In Figure 3a, the 33 GHz reflectivity is greater than the 95 GHz reflectivity as expected due to the higher extinction suffered by the W band from the suspended water droplets. Figure 3b depicts the difference of the 33 GHz and 95 GHz reflectivity, or DWR. From this, we computed the differential extinction, DE (see Fig. 3c), needed to estimate the cloud liquid content. Finally, in Figure 3d we present the liquid water content retrieved from profile scanned at 78 degrees elevation angle.

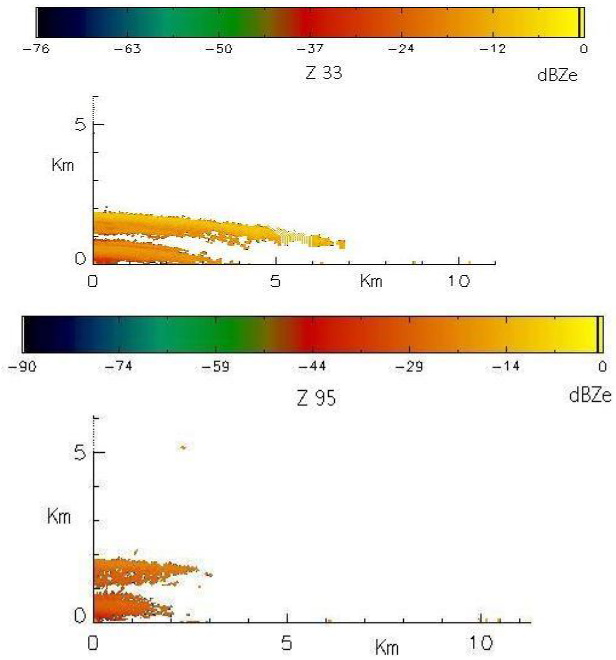

Fig. 2: Cloud's radar reflectivity for the 33 and 95 GHz from a stratus cloud obtained on March 17th, 2000 obtained with the CPRS.

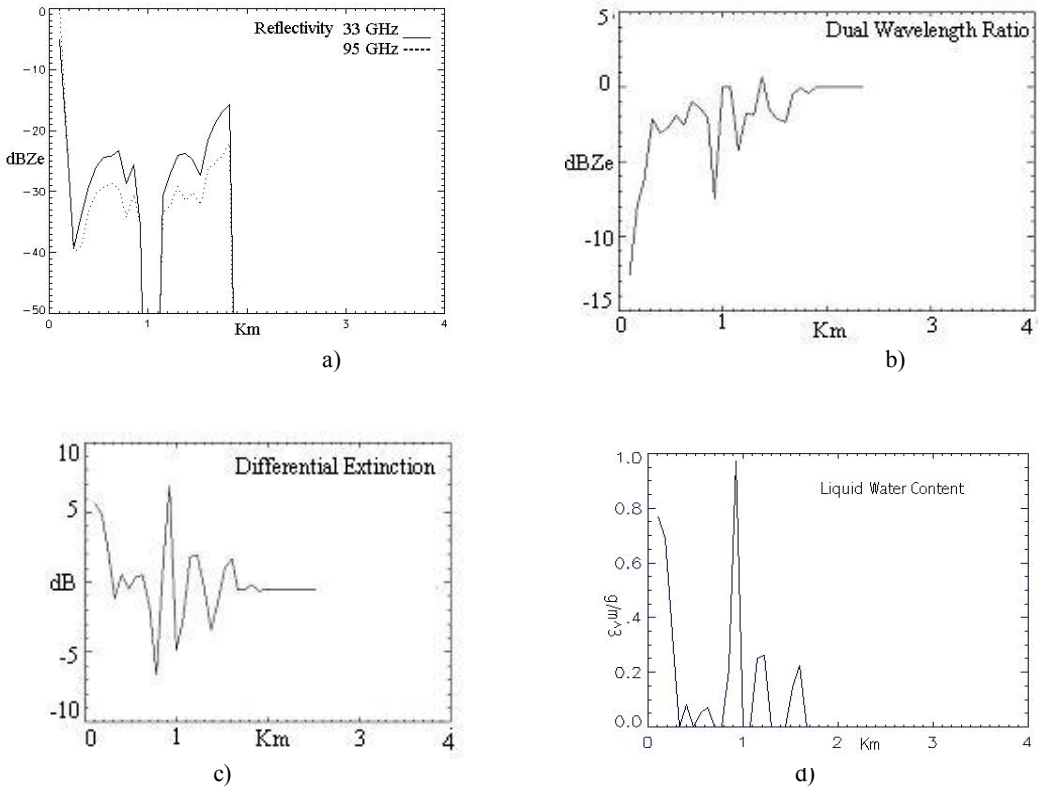

Fig. 3: a) Cloud's radar reflectivity for the 33 GHz and 95 GHz channels at 78 degrees. It shows the radar reflectivity after atmospheric attenuation is removed therefore both traces is very similar. b) Dual wavelength ratio at 78 degrees. c) Differential extinction at 78 degrees. d) Cloud's liquid water content at 78 degrees. It shows the liquid water content with several peaks that represents the cloud's more dense regions.

2.3 Data Processing and Correction

Several uncertainties arise when the radar is scanning a target. These uncertainties were analyzed and are explained in this following section. One uncertainty is the velocity the cloud is moving with respect to the velocity of the scanning radar. Another is the different cloud volumes the radars are sampling because of the different beamwidths that both radars have. In addition, there is the uncertainty added by the pulse shape, which is not a perfect square pulse.

2.3.1 Wind Correction

To determine if a wind correction was necessary we computed the wind velocity per layer. This was done to verify if the cloud was moving much faster than the radar was scanning and sampling. The radar beam was directed toward 220 degrees from North.

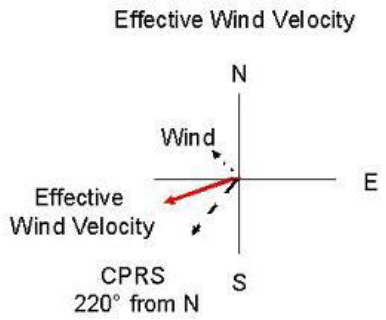

Fig. 4: Effective wind velocity vector.

In Figure 4, we can see the radar beam direction (dash), and the wind direction (dotted). The effective wind velocity was computed using the localization of the radar, and the angle between the wind and the radar, by using

$$A \bullet B = \vec{A}\vec{B}\cos\theta \tag{22}$$

where A represents the wind vector, B represents the radar position, and θ is the angle between both vectors.

The effective wind velocity was computed, up to 5 Km because stratus clouds are located at the lower part of the atmosphere. The radar angular velocity is 1.13°/sec. It was found that the cloud velocity was small enough so the radar is observing that same volume while completing one scan and no correction was necessary.

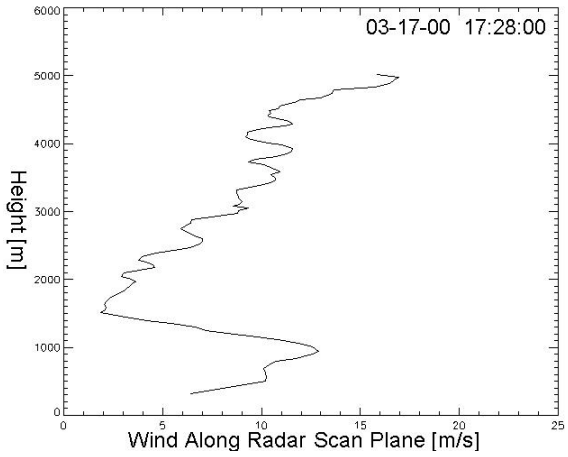

Fig. 5: Effective wind velocity.

2.3.2 Azimuth Correction

The radar reflectivity is processed in angles and range bins, where each angle represents the angle that the radar scanned and each range gate is each range cell where the radar received data. The effect scanning beamwidth is found from

$$erf(2\sqrt{\ln 4}\,\frac{\varphi}{\theta_1}) - erf[2\sqrt{\ln 4}\,\frac{(\varphi - \alpha MT_s)}{\theta_1} - \frac{1}{2}erf(\frac{\sqrt{\ln 4}\alpha MT_s}{\theta_1}) = 0 \tag{23}$$

which has two solutions φ_1 and φ_2 that determine the effective pattern width $\varphi_a = \varphi_2 - \varphi_1$, where φ is the one-way half-power beamwidth, M is the number of signal samples, T_s is the pulse repetition time, and α is the antenna rotation rate. It is very important to note that the 33 GHz beamwidth is 0.18 degrees and the 95 GHz is 0.06 degrees, which is three times smaller than the 33 GHz.

Because the effective scanning beamwidth of the 33 GHz radar is three times greater than the 95 GHz radar effective beamwidth, they are not measuring the same cloud volume. Consequently, an azimuth correction to the radar reflectivity was necessary. This correction was made by averaging three scan angles of the 95 GHz radar by one angle of the 33 GHz radar. After this, the 95 GHz radar reflectivity was smoothed in IDL.

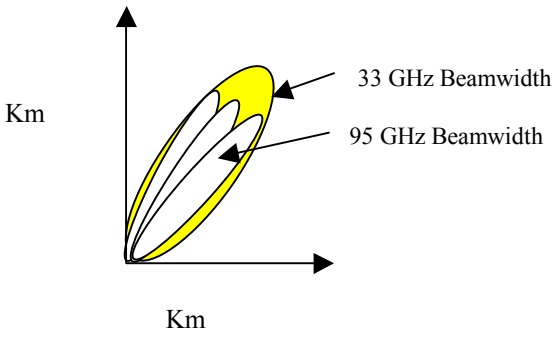

Fig. 6: Visualization of the differences in effective scanning beamwidth for both frequencies. The 33 GHz beamwidth is 0.18 degrees and the 95 GHz is 0.06 degrees, which is three times smaller than the 33 GHz.

2.3.3 Range Correction

For the range correction we need the time waveform of both radars, which is given by [16]:

$$W(t) = \frac{1}{2} I_0 \left\{ erf\left[aB_6(t + \frac{\tau}{2}) \right] - erf\left[aB_6(t - \frac{\tau}{2}) \right] \right\} \tag{24}$$

where I_0 is the prefilter amplitude $\frac{A}{\sqrt{2}}$ of a rectangular echo pulse having width τ; $a = \frac{\pi}{2\sqrt{\ln 2}}$; B_6 is the receiver-filter bandwidth, 6 dB width; erf is the error function, given by $erf(x) = \frac{2}{\sqrt{\pi}} \int_0^x e^{-t^2} dt$ and t=0 is the time at which the output echo is maximum and for the CPRS τ is equal to 500 x 10^{-9}.

$$l_r \equiv \frac{\frac{c\tau}{2}}{\int_0^\infty |W(r)|^2 dr} \tag{25}$$

where l_r is the finite bandwidth loss factor, range dependent; W is the range weighting function given by $dr = (t_2 - t_1)c$.

Next a convolution between the W-band data and K_a range weighting function and the K_a-band data with the range weighting function was performed on the data.

2.4 Corrected Scan Profiles

The corrected scanned radar reflectivity and DWR are shown in Figures 7a and 7b.

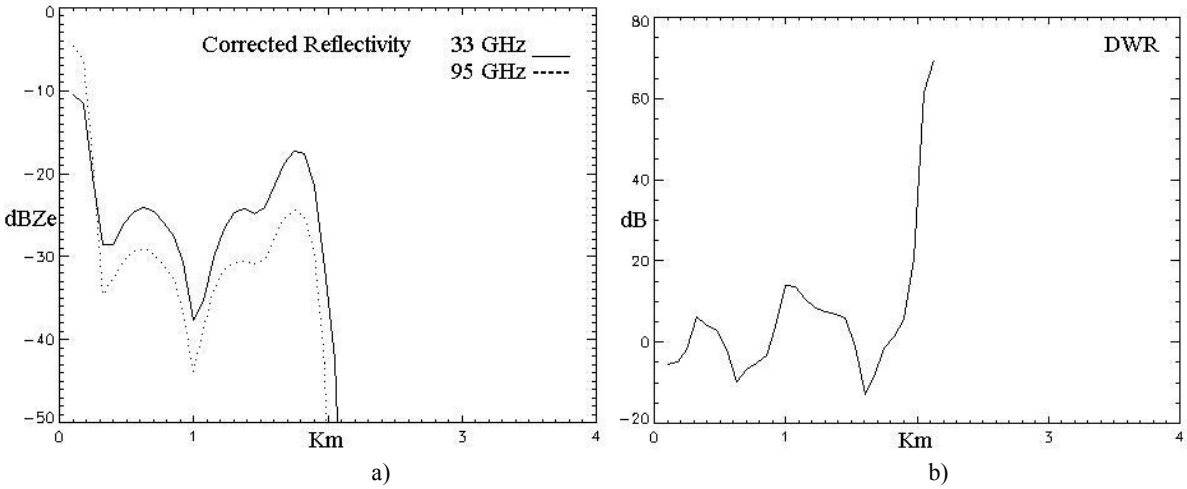

a) b)

Fig. 7: a) Corrected 33 GHz and 95 GHz reflectivity. b) Corrected DWR or dual wavelength ratio.

In the figure above, we can see the traces of the corrected by 33 GHz and 95 GHz reflectivity; and the DWR. It can be seen the improvement in the traces, comparing with Figures 3a and 3b. From these, the effective diameter (D_0) and the particle number density (N_0) were estimated. These are the only two parameters needed to determine N(D).

$$N(D) = N_0 e^{-\frac{3.67D}{D_0}} \tag{26}$$

By using the cloud's radar reflectivity and the liquid water content, derived from the DWR, DE and the air temperature, two products were obtained, D_0 and N_0, using equations [16]

$$Z = \int_0^\infty N(D) D^6 dD \tag{27}$$

$$LWC = \frac{\pi \rho_w}{6} \int_0^\infty N(D) D^3 dD \tag{28}$$

where D is the drop size in mm, D_0 is the effective drop size diameter in mm, N_0 is a constant in $mm^{-1}\ m^{-3}$, ρ_w is the water density of the drop 10^3 kg m^{-3}, Z is the reflectivity in mm^6, and the liquid water content in kg m^{-3}. N_0 and D_0 were found by using Newton's iterative method for solving a nonlinear system of equations [15].

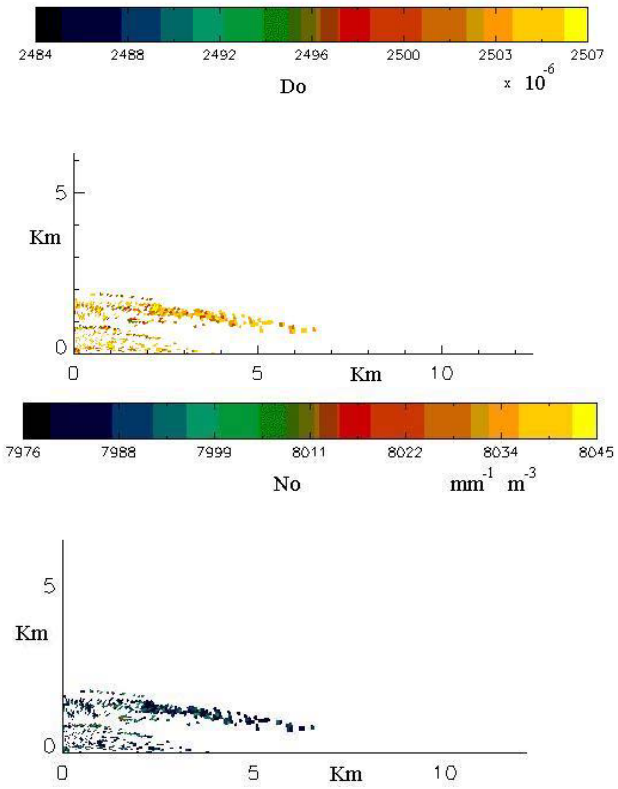

Fig. 8: a) D_0 values for the stratus cloud. It varies from 2.481 to 2.507 μm. b) N_0 values for the stratus cloud. It varies from 7976 to 8055 $mm^{-1}\ m^{-3}$.

Figures 8a and 8b show the resulting values for the drop size distribution inside the stratus clouds. We obtained values of mean drop diameter from 2.48 to 2.51 μm and values for the peak number concentration of 7,976 to 8,055. These values agree with Marshall and Palmer distribution for this type of cloud, i.e. D_0 = 2.5 μm and N_0 = 8,000.

CONCLUSIONS

Cloud reflectivity measurements collected by dual wavelength radar can be used to estimate the microphysical properties of clouds such as the median size diameter, the particle size distribution, the peak number concentration, the cloud's water density, and the atmospheric extinction. This method is less affected by atmospheric attenuation than radiometers and lidars [17-18] that are greatly affected by the large optical depths and atmospheric attenuation.

The reflectivity data was corrected in three ways to diminish the presence of uncertainties. Correction by wind was not necessary because the cloud was moving slower than the radar's scan velocity. The azimuth correction was done to account for the differences in effective scanning angles at each band. There is a clear improvement in the W-band reflectivity and in the 33-band reflectivity and in the DWR after correcting by range gates and azimuth.

Also, the drop size distribution as well as the peak number concentration was estimated using Newton's method for non-linear system of equations. The values of D_0 range from 7,976 to 8,055 m-3 mm-1 and D_0 ranges from 2.481 to 2.507 μm. These D0 values agree with previous models of stratus clouds [19]. The values obtained in this work for the drop size distribution parameters within the stratus cloud, No and Do, were in excellent agreement with the model by Marshall and Palmer.

ACKNOWLEDGEMENTS

This work is supported by the Center for CLloud Microwave Measurements of ATmospheric Events (NASA Grant number NAG102074) and to the Tropical Center for Earth Space Studies (NASA Grant number NCC5-518).

REFERENCES

1. F. K. Lutgens, and E. L. Tarbuck, *The Atmosphere*, Chapter 5, Seventh Edition, 1998 Prentice Hall.
2. S. M. Sekelsky, R. E. McIntosh, W. L. Ecklund, and K. S. Gage, "Cloud Observations with a Polarimetric 33 GHz and 95 GHz Radar", Meteorology and Atmospheric Physics, **58**:123-140, 1996
3. J. M. Firda, S. M. Sekelsky and R. E. McIntosh, "Application of Dual-Frequency Millimeter-Wave Doppler Spectra for the Retrieval of Drop Size Distributions and Vertical Air Motion in Rain", Journal of Atmospheric and Oceanic Technology, **16**:216-235, 1999
4. S. M. Sekelsky, W. L. Ecklund, J. M. Firda, K. S. Gage, R. E. McIntosh, "Particle Size estimation in Ice-Phase Clouds Using Multifrequency Radar Reflectivity Measurements at 95, 33, and 2.8 GHz", American Meteorological Society, 5-28, January 1999
5. T. H. Vonder, K. R. Dean, J. M. Forythe, T. J. Greenwalds, and S. Q. Kidder, "Comparison of Satellite and Ground Based Measurements of Cloud Liquid Water in Several Climate Zones", *Proceedings of IGARSS '01, IEEE 2001 International,* **2**, *pp. 688 -690*
6. S. Cruz-Pol, S. M. Sekelsky, and N. Colon, "Multi-Dimensional Cloud Images Retrieval From Ground-Based Radar Operating At Millimeter Wave Frequencies", *Proceedings of IGARSS '01. IEEE 2001 International,* **6**, *pp: 2642 -2644*
7. S. Cruz-Pol, "An Improved Model for the Microwave Brightness Temperature Seen From Space Over Calm Ocean", A Thesis in Electrical Engineering, Pennsylvania State University, 1998
8. P. W. Rosenkranz, "Shape of the 5 mm Oxygen Band in the Atmosphere" *IEEE Trans. Ant. Prop*., AP-23, 498-506, 1975
9. H. J. Liebe, "MPM-An Atmospheric Millimeter-Wave Propagation Model", International *Journal of Infrared and Millimeter Waves*, **10**, no. 6, 1989
10. R. J. Donaldson Jr., "The Measurement of Cloud Liquid-Water Content by Radar", *Journal of Meteorology*, **12**, pp. 238-245, 1955
11. H. J. Liebe, and D. H. Layton, "Millimeter-waves Properties of the Atmosphere: Laboratory Studies and Propagation Modeling", Nat. Telecom. And Inform. Admin., Boulder, CO, NIT Rep. 87-24
12. P. W. Rosenkranz, "Absorption of Microwaves by Atmospheric Gases", *Atmospheric Remote Sensing by Microwave Radiometry*, Chapter 2, Edition by Janssen, Wiley, NY, 1993
13. S. J. Keihm, V. Zlotnicki, and C. S. Ruf, "TOPEX Microwave Radiometer Performance Evaluation", *IEEE Trans. Geosci. And Remote Sens*. 2000, **38**, No. 3, pp. 1379-1386
14. S. M. Sekeslky, "Multifrequency Radar Observations of Liquid Clouds", *Proceedings of IGARSS 2000 IEEE 2000,* **5**, *pp. 1807-1809*
15. R. L. Burden, and J. D. Faires, *Numerical Analysis*, Chapter 10, Fourth Edition, 1989 PWS- Kent Publishing Company.
16. R. J. Doviak, and D. S. Zrnic, *Doppler Radar and Weather Observations,* Chapters 4, 7 and 8, Second Edition, 1993 Academic Press.
17. S. Y. Matrosov, "Radar Reflectivity in Snowfall*", IEEE Trans. Geosci. Remote Sens*.1992, **30**, 454-461
18. J. M. Intrieri, G. L. Stephens, W. L. Eberhard, and T. Uttal, "A Method for Determining Cirrus Cloud Particle Sizes Using Lidar and Backscatter Techinique*", J. Appl. Meteor*.1993, **32**, 1074-1082
19. J. S. Marshall, and W. Palmer, "The distributions of raindrops with size", *J. Meteorol*., 1948, **5**, 165-166